

W MASS AND W^+W^- FINAL STATE INTERACTIONS

NIGEL K. WATSON

*School of Physics and Astronomy, University of Birmingham,
Edgbaston, Birmingham, B15 2TT, Great Britain*



Precise measurements of the mass and width of the W boson are carried out in e^+e^- collisions at LEP, by kinematic reconstruction of the invariant mass distributions of $W^+W^- \rightarrow q\bar{q}'\ell\bar{\nu}_\ell$ and $W^+W^- \rightarrow q\bar{q}'q\bar{q}'$ candidate events. The most recent combination of such results from ALEPH, DELPHI, L3 and OPAL uses approximately 82% of the final LEP2 integrated luminosity and is preliminary. The mass of the W boson so determined is $M_W = 80.446 \pm 0.026 \pm 0.030$ GeV, while the corresponding direct measurement of the W boson width gives $\Gamma_W = 2.148 \pm 0.071 \pm 0.063$ GeV. These measurements are subject to sizeable systematic uncertainties from the QCD phenomena of Bose-Einstein correlations and colour reconnection. Recent substantial progress in both of these areas is reported.

1 W Mass and Width

The LEP e^+e^- collider at CERN has provided an ideal environment for the study of the properties of the gauge bosons of the Standard Model of electroweak interactions. Since 1996, it operated at centre-of-mass energies above the W^+W^- production threshold (LEP2), allowing direct measurements of the W boson mass, M_W . When combined with the direct measurements of the top quark mass at the Tevatron, these allow further constraints to be set on the mass of the Higgs boson via electroweak radiative corrections. Comparison between the direct measurements of the mass of the W boson and the value determined indirectly from data recorded at $\sqrt{s} \approx M_Z$ provides an important test of the self-consistency of the Standard Model. The direct measurement of Γ_W further tests the consistency of the Standard Model.

The measurement of M_W and Γ_W is divided into three stages: selection of W^+W^- events, event-by-event mass reconstruction, and determination of M_W itself.

1.1 W^+W^- Final States

W^+W^- events are divided into three final states. $W^+W^- \rightarrow q\bar{q}'q\bar{q}'$ events comprise 45% of the total W^+W^- cross-section and are characterised by four energetic jets of hadrons with little or no missing energy. Semi-leptonic $W^+W^- \rightarrow q\bar{q}'\ell\bar{\nu}_\ell$ decays comprise 44% of the total W^+W^- cross-section and are characterised by two distinct hadronic jets, a high-momentum lepton and missing momentum due to the prompt neutrino from the leptonic W decay. The signature for the $W^+W^- \rightarrow q\bar{q}'\tau\nu_\tau$ channel is similar, with the exception that the τ lepton is identified as an isolated, low-multiplicity jet typically consisting of one or three tracks. The $W^+W^- \rightarrow \ell^+\nu_\ell\ell^-\bar{\nu}_\ell$ channel, with at least two unobserved neutrinos and a relatively low branching fraction, has limited M_W sensitivity and is not discussed herein.

1.2 Invariant Mass Reconstruction

The clean environment at LEP allows a complete kinematic reconstruction of the invariant mass on an event-by-event basis. Hadrons are grouped together into jets using clustering algorithms such as k_\perp . In $W^+W^- \rightarrow q\bar{q}'\ell\bar{\nu}_\ell$ events, charged leptons are identified and neutrinos are inferred from the missing energy and momentum. The invariant masses of the two W bosons can be determined directly from the reconstructed momenta of observed decay products. Experimentally, the limiting factor in the mass resolution is the uncertainty in the jet energy measurement, which is poor in contrast to the measured jet directions. As the centre-of-mass energy is well known, the mass resolution can be improved significantly (factor $\sim 2\text{--}3$) by use of a constrained kinematic fit imposing the four constraints of energy and momentum conservation (4-C fit). Small additional gains are possible by imposing the additional constraint that the masses of the two W bosons are equal in each event (5-C fit), giving a single mass measurement per event.

For $W^+W^- \rightarrow q\bar{q}'\ell\bar{\nu}_\ell$ events, the number of effective constraints is reduced to 2 (1) for a 5-C (4-C) fit due to the three missing degrees of freedom corresponding to the unmeasured neutrino momentum. For $W^+W^- \rightarrow q\bar{q}'\tau\nu_\tau$ events, most of the mass information is given by the hadronically decaying W . A frequent assumption in constructing kinematic fits for these events is that the true τ direction coincides with its observed decay products, while the τ energy is unknown, removing a further constraint.

In $W^+W^- \rightarrow q\bar{q}'q\bar{q}'$ events where four jets are reconstructed, there are three possible pairwise combinations. In some analyses, a single preferred combination is selected on the basis of information such as kinematic fit probabilities, jet-jet angles or the CC03^a matrix elements. In other analyses, all combinations are used with different weights assigned to each, or two combinations are used with equal weight. In addition, as quarks may radiate energetic gluons leading to a distinct five-jet topology, several analyses separate events into four- and five-jet categories to be treated separately, leading to an overall improved mass resolution.

1.3 M_W Determination

There are three main methods whereby M_W is determined. The most widely used (ALEPH, L3, OPAL) involves reweighting Monte Carlo events including detector simulation to an arbitrary value of M_W using the ratio of 4-fermion or CC03 matrix elements. A likelihood fit to the reweighted mass spectra determines the value of M_W which best resembles the data. The fit can be either a 1-dimensional fit to the 5-C fit mass, possibly performed in several exclusive regions of reconstructed mass error, or a 2-dimensional fit to the 4-C fit masses. There is an implicit MC correction, e.g. for effects such as initial state photon radiation (ISR) and detector effects.

A second method (DELPHI, OPAL) constructs an event likelihood from the convolution of a Breit-Wigner with a radiator function (to account for ISR) and a resolution function (to account

^a Doubly-resonant W^+W^- production diagrams, *i.e.* t -channel ν_e exchange and s -channel Z^0/γ exchange.

for detector effects). The probability of an event being W^+W^- is also included in the likelihood. These ‘convolution’ based methods make more use of the information per event and so might be expected to give a more precise M_W determination. An explicit bias correction has to be applied to the fitted M_W , based on events including detector simulation.

The third method (OPAL) fits an analytic function (asymmetric Breit-Wigner) to the reconstructed mass spectra. Similarly, an explicit bias correction is made. All methods yield comparable precision on the measured M_W .

1.4 Systematic Effects

Source	Uncertainty on M_W (MeV)		
	$q\bar{q}'\ell\bar{\nu}_\ell$	$q\bar{q}'q\bar{q}'$	Combined
ISR/FSR	8	8	7
Hadronisation	19	17	18
Detector	11	8	10
Beam Energy	17	17	17
Colour Reconnection	—	40	11
Bose-Einstein Correlations	—	25	7
Other	4	5	3
Total systematic	29	54	30
Statistical	33	31	26
Total	44	63	40

Table 1: Summary of the systematic uncertainties for the combined LEP fit results.

The statistical uncertainty on the combined LEP M_W measurements is 26 MeV, therefore a clear understanding of systematic uncertainties is vitally important. Systematics may be correlated between combinations of experiments, channels and years of data taking. A summary of the uncertainties, without giving the detailed decomposition into the various correlated sources, is given in Table 1. A consequence of the large systematics from Bose-Einstein Correlations (BEC) and Colour Reconnection (CR) is that the $W^+W^- \rightarrow q\bar{q}'q\bar{q}'$ channel has a reduced contribution to the overall M_W , with a weight of 0.27. In the case where both channels had equal weight, the statistical uncertainty on M_W would be reduced by $\sim 15\%$.

The most significant systematics are those which are correlated between experiments, as described below. Photonic radiative corrections (ISR, FSR) have been estimated originally by comparing different ISR models, *e.g.* as in KORALW and EXCALIBUR. More recently, KORALW events have been reweighted to correspond to an $\mathcal{O}(\alpha^2)$ or $\mathcal{O}(\alpha)$ treatment of ISR using the matrix elements calculated inside the model (the default calculation is at $\mathcal{O}(\alpha^3)$). However, these calculations are incomplete at $\mathcal{O}(\alpha)$ (no ISR/FSR interference, or direct γ radiation from Ws), so ideally a complete calculation as in the Double Pole Approximation of RacoonWW would be used. As yet, this only produces weighted events so no realistic estimates are available.

Hadronisation has been estimated by comparing models, *e.g.* JETSET and HERWIG. Other approaches include reweighting key variables in MC to correspond to data and propagating the effect to M_W . DELPHI also advocate the use of so-called ‘mixed Lorentz boosted Z^0 ’ (MLBZ).

The relative uncertainty in the LEP beam energy enters directly into the uncertainty in M_W , due to the use of kinematic fits which include a constraint to the centre-of-mass energy. Uncertainties in beam energy are taken directly from the detailed studies of resonant depolarisation, NMR probes/flux loop measurements, and the LEP spectrometer project.

A significant bias to the apparent W mass measured in the $W^+W^- \rightarrow q\bar{q}'q\bar{q}'$ channel could arise if the hadronisation of the two W bosons is not independent and correctly modelled. Final

state interactions such as CR and BEC may cause just this effect and are estimated by using phenomenological models. Direct searches for these effects, which may limit the viable set of such models, are described below

2 Colour Reconnection

In $W^+W^- \rightarrow q\bar{q}'q\bar{q}'$ events, the products of the W decays in general have a significant space-time overlap as the separation of their decay vertices is small compared to characteristic hadronic distance scales. Colour reconnection refers to a rearrangement of the colour flow between the two W bosons. The effects of interactions between the colour singlets during the perturbative phase are expected to be small, $\sim (\frac{\alpha_s}{\pi N_{colours}})^2 \Gamma_W$. The situation is less clear in the non-perturbative phase, where phenomenological models are implemented in hadronic Monte Carlos. A higher susceptibility to CR (and more $Z^0/\gamma \rightarrow q\bar{q}$ background) is expected when W^+ and W^- hadronisation regions overlap, so the spacetime picture of the QCD shower development is important.

The predicted (barely) observable effects of CR include changes to the charged particle multiplicity, momentum distributions and the particle flow relative to the 4-jet topology. The aim is to establish whether CR actually exists as well as controlling (or better, calibrating using data) the bias on M_W measurements. The basic analysis method consists of comparing fully hadronic events with either: models with/without CR; $W^+W^- \rightarrow q\bar{q}'\ell\bar{\nu}_\ell$ events; or MLBZs.

2.1 Charged Particle Multiplicity

Expt.	$\langle n_{ch}^{4q} \rangle$	$\langle n_{ch}^{qq\ell\nu} \rangle$	$\Delta \langle n_{ch} \rangle$
ALEPH (183–202 GeV) ¹	35.75 ± 0.54	17.41 ± 0.19	$+0.98 \pm 0.43$
DELPHI (183 GeV) ²	38.11 ± 0.72	19.78 ± 0.65	$\langle n_{ch}^{4q} \rangle / 2 \langle n_{ch}^{qq\ell\nu} \rangle$
DELPHI (189 GeV) ²	39.12 ± 0.49	19.49 ± 0.41	$= 0.981 \pm 0.027$
L3 (183–202 GeV) ³	37.90 ± 0.43	19.09 ± 0.24	-0.29 ± 0.40
OPAL (183 GeV) ⁴	39.4 ± 0.8	19.3 ± 0.4	$+0.7 \pm 1.0$
OPAL (189 GeV) ⁴	38.31 ± 0.44	19.23 ± 0.27	-0.15 ± 0.58

Table 2: Summary of recent charged particle multiplicity measurements, with combined statistical and systematic errors. ALEPH measurements are not corrected for detector effects.

The difference in multiplicities between $W^+W^- \rightarrow q\bar{q}'q\bar{q}'$ and twice the hadronic component of $W^+W^- \rightarrow q\bar{q}'\ell\bar{\nu}_\ell$ events, $\Delta \langle n_{ch} \rangle = \langle n_{ch}^{4q} \rangle - 2 \langle n_{ch}^{qq\ell\nu} \rangle$, should be zero in the absence of CR effects. A compilation of the most recent multiplicity measurements is given in Table 2. The effects are expected to be enhanced for softer particles, $p \lesssim \Gamma_W$, so observables with implicit scale such as $\ln(1/x_p)$, p_T , rapidity, have also been studied with similarly inconclusive results. As the systematics are now comparable to the statistical uncertainties, no attempt is made to combine results in a trivial way. DELPHI and OPAL have studied the effects of CR for heavier hadron species, such as kaons and protons. Although the numerical effects of CR are larger, the significance is reduced due to loss in statistical precision.

2.2 Interjet Analysis

These analyses^{1, 3, 4}, are based on the “string effect” analysis in $e^+e^- \rightarrow q\bar{q}g$ at lower energies. All LEP collaborations are now using these analyses, recently developed by L3 and following earlier studies⁵. Events are selected by requiring, in addition to usual $W^+W^- \rightarrow q\bar{q}'q\bar{q}'$ criteria: four distinct jets ($y_{34} > 0.01$ in k_\perp scheme); the two largest jet-jet angles are 100° – 140° (intra- W regions); the two smallest jet-jet angles are $< 100^\circ$ (inter- W regions) and have no jets in

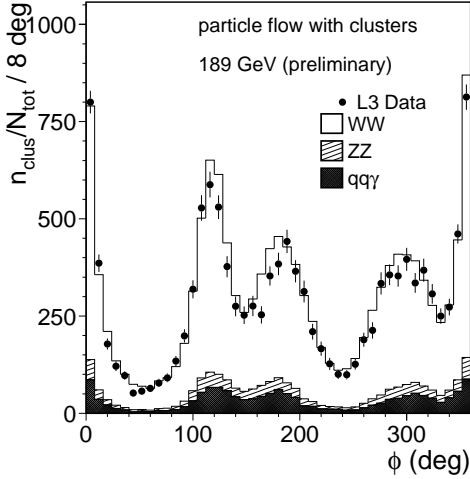


Figure 1: Particle density in a single di-jet plane.

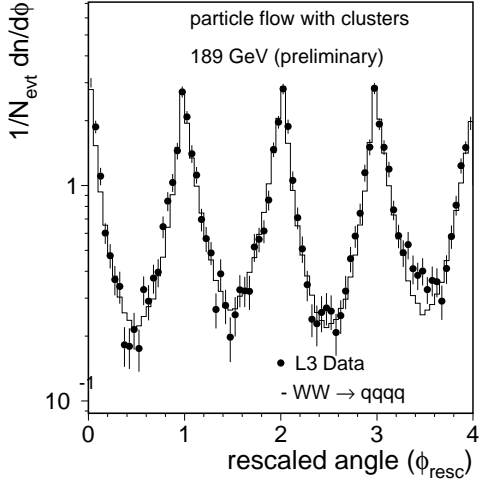


Figure 2: Particle density for all planes, scaled to di-jet opening angles.

common. This leads to an efficiency $\sim 15\%$, good jet-jet to W association, with “strings” that are back-to-back and not crossing one another in 87% of events. In the case of L3 at $\sqrt{s} = 189$ GeV, 209 such events are selected. Next, particles are projected onto each of the four selected di-jet planes, forming the particle density as a function of angle from one of the plane defining jets. This is illustrated in Figure 1, where the inter-W regions correspond to the larger regions between the jet peaks. As the di-jet angles vary from event to event and plane to plane, particle densities are scaled to the di-jet opening angle event-by-event, as shown in Figure 2, after background subtraction.

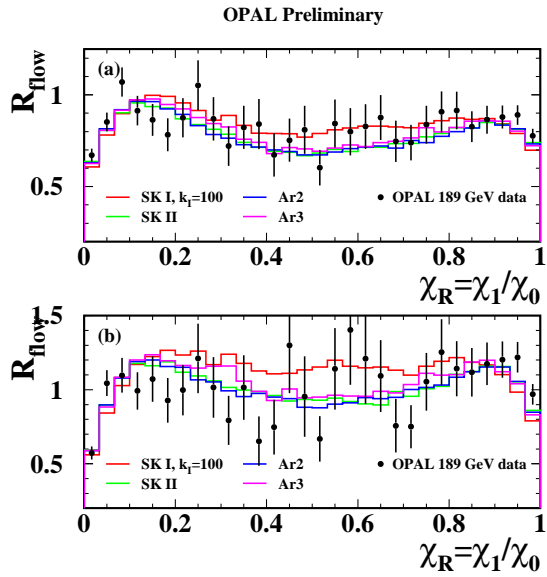


Figure 3: Ratio of inter-W/intra-W particle flow (a) higher efficiency analysis, weighted by $\ln \frac{1}{x_p}$, (b) L3-like selection, see⁴ for details.

To quantify the effects, the ratio of the inter-W/intra-W regions (or its inverse) is formed, as shown in Figure 3, and integrated in the central region away from the jet peaks. An alternative is to consider the ratio of the integrals of inter-W and intra-W particle densities. L3 estimate their sensitivity to the SK I CR model⁶, is 3.2 (0.5) σ total error for 100 (32) % reconnected events, using $\frac{1}{3}$ of their LEP2 sample. OPAL have a variant on the analysis using a likelihood based selection to associate di-jets with Ws, a 4-C kinematic fit to define jet axes, and no double counting of particles, which predicts a slight improvement in sensitivity and favours $\sim 65\%$ of events reconnected in the SK I model. However, their emulation of the L3 analysis prefers a no-CR scenario.

2.3 Towards Mass Biases

In the SK I model, the reconnection probability is a free parameter and therefore can be adjusted to provide the best agreement of data. L3 estimate their data prefer $\sim 40\%$ CR in this model,

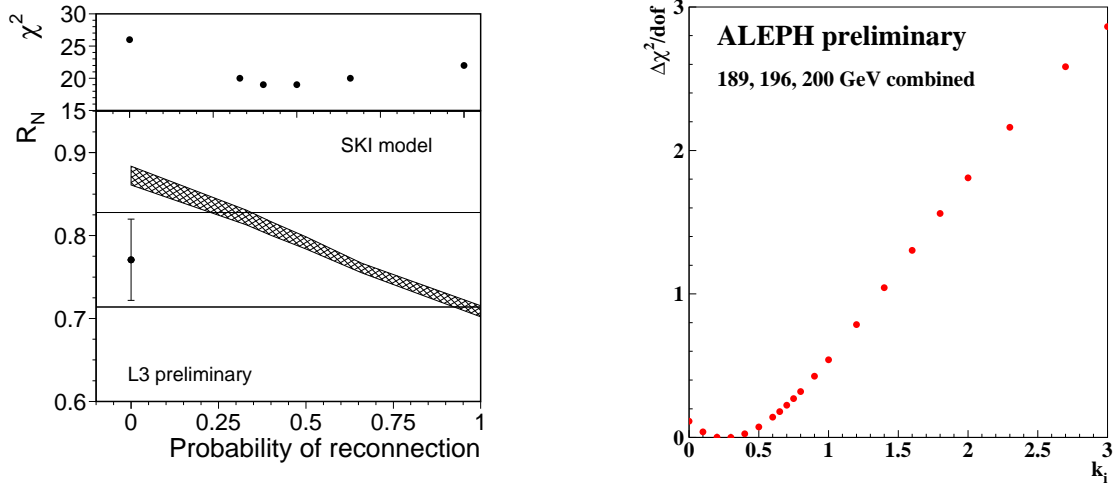


Figure 4: χ^2 between data and SK CR model as a function of reconnection probability.

and are 1.7σ separated from no-CR scenario, as shown in Figure 4. A similar study in ALEPH suggests data prefer this model dependent probability to be $\sim 15\%$, also shown in Figure 4. Having estimated the preferred CR probability, it is trivial to estimate the corresponding bias on M_W in the context of a single model. Comparison of such results between collaborations is complicated by differences in the models they use, such as hadronisation tuning. Using common samples of simulated events which are processed by each collaboration’s detector simulation is in progress and will lead to a significant improvement in understanding in this area.

3 Bose-Einstein Correlations

Bose-Einstein correlation leads to the enhanced production of identical boson pairs, such as $\pi^+\pi^+$ or $\pi^-\pi^-$, at small 4-momentum difference, $Q^2 = -(\mathbf{p}_1 - \mathbf{p}_2)^2$. This phenomena is firmly established in various environments, in $Z^0/\gamma \rightarrow q\bar{q}$ at LEP1 and between the particles of a single W boson at LEP2, among others. Traditionally, it is studied using a 2-particle correlation function: $R(\mathbf{p}_1, \mathbf{p}_2) = \rho_2(\mathbf{p}_1, \mathbf{p}_2)/\rho_0(\mathbf{p}_1, \mathbf{p}_2)$, where ρ_2 and ρ_0 are 2-particle densities with and without BEC, respectively. Of particular interest in the W^+W^- case is whether or not there is any additional correlation introduced between the decay products of the two Ws, which could potentially bias M_W measurements.

One serious problem in this area is the construction of the reference sample, ρ_0 , and there are three frequently used methods. The first takes unlike-sign particle species, such as $\pi^+\pi^-$, forms the ratio of like-sign/unlike-sign, and then takes the ratio of this quantity relative to Monte Carlo to reduce the impact of having resonances in ρ_0 but not in ρ_2 (“double ratio”). The second consists of taking ρ_0 to be a like-sign MC sample, although this is subject to deficiencies in modelling. The third involves mixing pairs of data events, such as $Z^0/\gamma \rightarrow q\bar{q}$ or the hadronically decaying W in $W^+W^- \rightarrow q\bar{q}'\ell\bar{\nu}_\ell$. Another serious problem is the ignorance of non-perturbative QCD amplitudes, forcing analyses to resort to MC models, which in turn suffer from being probabilistic in nature, with the models of BEC implemented in Monte Carlo simulations.

A common parametrisation of the correlation function is $R(Q) \sim 1 + \lambda \exp(-r^2 Q^2)$, where λ and r represent the source strength and size, respectively. Results from each of ALEPH¹, L3³ and OPAL⁴ are summarised below. No DELPHI results were presented (at their request), as they were undergoing substantial revision. Results which differed qualitatively from their earlier analyses were presented at Moriond QCD 2001.

In the OPAL analysis, the two-particle correlation function is formed using the double ratio of like-sign/unlike-sign, data/no-BEC MC. Three event classes are identified, $W^+W^- \rightarrow q\bar{q}'\bar{q}\bar{q}'$

$W^+W^- \rightarrow q\bar{q}'\ell\bar{\nu}_\ell$ and $Z^0/\gamma \rightarrow q\bar{q}$, each consisting of the linear sum of pure contributions weighted by a probability derived from MC. The classes are C^{DIFF} (inter-W BEC), C^{SAME} (intra-W BEC), C^{Z^*} (non-radiative $q\bar{q}$). A simultaneous fit is performed to extract λ^{DIFF} for various source size hypotheses. Examples are: $R^{DIFF} = R^{SAME} = R^{Z^*}$, yielding $\lambda^{DIFF} = -0.14 \pm 0.36$, and completely independent R_s , giving $\lambda^{DIFF} = 2.9 \pm 1.7$ and $\lambda^{SAME} = 0.62 \pm 0.10$. Intra-W BEC is established, but the analysis is unable to ascertain whether inter-W BEC exist.

In the ALEPH analysis, again the double ratio is used, and the $Z^0/\gamma \rightarrow q\bar{q}$ background, in which BEC are known to be present, is modelled using the model BE_3 . It is concluded that inter-W BEC is disfavoured by data with a significance of 2.2σ , while the data are compatible with intra-W BEC. An event mixing analysis is also used, which qualitatively disfavours inter-W BEC, but is as yet incomplete in that a full study of systematic errors has not been performed.

The L3 analysis uses the method of Chekanov *et al.*⁷, which sets out a very robust framework to test for the presence of inter-W BEC. If the W^+ and W^- decays are uncorrelated, then:

$$\rho_2^{W^+W^-}(\mathbf{p}_1, \mathbf{p}_2) = \rho_2^{W^+}(\mathbf{p}_1, \mathbf{p}_2) + \rho_2^{W^-}(\mathbf{p}_1, \mathbf{p}_2) + 2\rho_1^{W^+}(\mathbf{p}_1)\rho_1^{W^-}(\mathbf{p}_2), \quad (1)$$

where the first two terms on the r.h.s. are estimated from individual $W^+W^- \rightarrow q\bar{q}'\ell\bar{\nu}_\ell$ events, assuming they are the same in W^+ and W^- decays, while the rightmost term is formed by mixing pairs of $W^+W^- \rightarrow q\bar{q}'\ell\bar{\nu}_\ell$ events to give “fake” events in which there can be no true inter-W BEC. All background samples include BEC using the BE_{32} model.

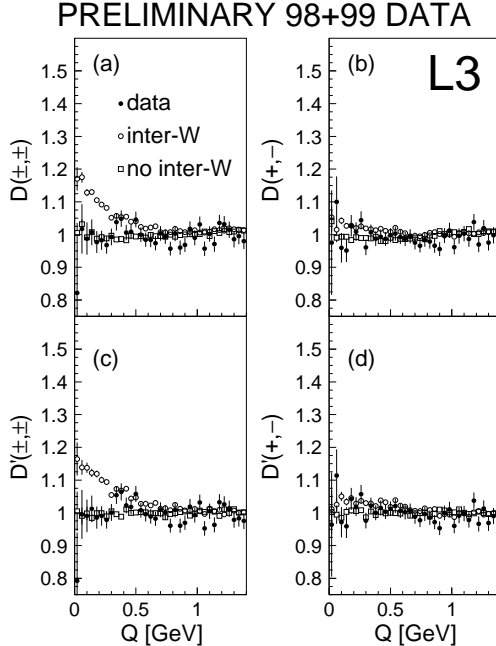


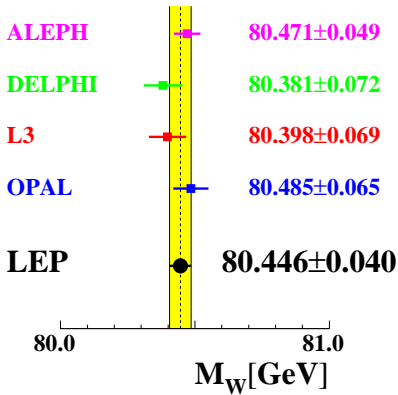
Figure 5: Inter-W BEC observables, see text for details.

The variable D is defined as the ratio of the left hand side to the right hand side of Equation 1. In the absence of inter-W correlations, such as from BEC, and of bias introduced in the event mixing, $D = 1$. To eliminate this potential residual experimental bias, the variable D' is constructed as ratio of D in data to that in MC (having only intra-W BEC). Figures 5(a)-(b) and 5(c)-(d) show the variables D for like-sign and unlike-sign data, and similarly for D' . The data clearly favour the no inter-W BEC model. By fitting the phenomenological correlation function to these data, L3 obtain $\lambda = 0.013 \pm 0.018 \pm 0.015$, where $\lambda = 0$ corresponds to no inter-W BEC. In contrast, the BE_{32} model gives $\lambda = 0.126 \pm 0.006(stat.)$, thus the data disfavour inter-W BEC by 4.7σ .

4 Combined LEP Results and Summary

Based on an analysis of 2.8 fb^{-1} ($\sim 82\%$ of the entire LEP2 data sample, 100% analysed by ALEPH and L3), the following preliminary measurements⁸, summarised in Figures 6 and 7, are made: $M_W = 80.446 \pm 0.026 \pm 0.030 \text{ GeV}$, $\Gamma_W = 2.148 \pm 0.071 \pm 0.063 \text{ GeV}$, $\Delta_{M_W}(q\bar{q}'q\bar{q}' - q\bar{q}'\ell\bar{\nu}_\ell) = +18 \pm 46 \text{ MeV}$. Further improvements in systematics are anticipated. Colour reconnection analyses, such as interjet multiplicity, from all collaborations will be combined. The overall conclusion regarding inter-W Bose-Einstein correlations among the LEP collaborations is finally becoming more consistent: there is increasingly strong evidence that they do not exist.

LEP Preliminary : Winter 2001



LEP Preliminary : Winter 2001

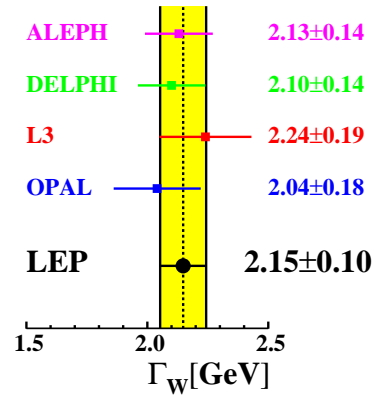


Figure 6: Combined LEP M_W and Γ_W , all channels.

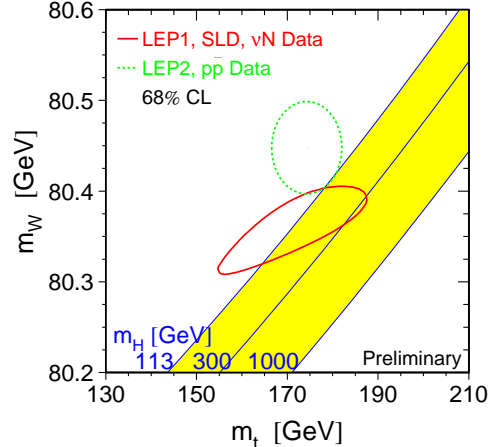
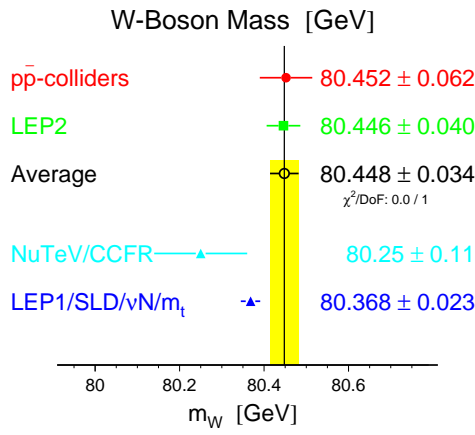


Figure 7: Comparison of LEP M_W with other measurements and Standard Model predictions

Acknowledgements

Work supported by PPARC grant GR/L04207. I would like to thank colleagues in all LEP collaborations for the preparation and timely combination of results presented.

References

1. ALEPH 2000-024; Phys. Lett. **B478** (2000) 50; ALEPH 2000-051; ALEPH 2000-058.
2. DELPHI Collab., Eur. Phys. J. **C18** (2000) 203.
3. L3 Collab., L3 Note 2615 (2-Mar-2001) L3 Note 2560 (5-Mar-2001);
4. OPAL Collab., PN393; Phys. Lett. **B453** (1999) 153; PN417; PN448.
5. CERN LEP2 Workshop, CERN 96-01, Vol. 1, p. 191, eds. G. Altarelli, T. Sjöstrand, F. Zwirner; A. Ballestrero *et al.*, J. Phys. G: Nucl. Part. Phys. **24** (1998) 365.
6. T. Sjöstrand and V.A. Khoze, Z. Phys. **C62** (1994) 281; Phys. Rev. Lett. **72** (1994) 28.
7. S.V. Chekanov, E.A. De Wolf, W. Kittel, Eur. Phys. J. **C6** (1999) 403.
8. LEP W^+W^- Working Group, combination for Winter 2001, <http://lepewwg.web.cern.ch/LEPEWWG/leppw/mw/Winter01/> and references therein.